Supplementary materials

Familial Turkish CIPO patients

The two brothers and sister, aged 26, 28 and 30 (IV-9; IV-10; IV-11, Figure 1A) presented with recurrent abdominal pain and pseudo-obstruction since childhood. The proband IV-10 presented with episodes suggestive of intestinal obstruction since childhood (11 years of age) and underwent repeated abdominal surgeries, although extensive investigation failed to detect any structural obstacle to transit. Endoscopic evaluation of the esophagus revealed a long-segment Barrett esophagus extending up to 18 cm, and no evident abnormalities in the stomach. Esophageal manometry revealed aperistalsis and undetectable lower esophageal pressures, and barium small-bowel enema showed megaduodenum and delayed emptying. He died at 29 years of age due to complications of a surgical procedure prompted by intestinal perforation, while he was on total parenteral nutrition.

His brother (IV-9) had a similar long-lasting history of multiple hospitalizations and surgical procedures due to recurrent sub-occlusive episodes. He presented virtually identical findings at upper gastrointestinal endoscopy and esophageal manometry. However, his clinical features also included otosclerosis, glaucoma, and epilepsy. Cardiac abnormalities included pulmonary and tricuspid valve insufficiency. Their sister IV-11 is a 30-year-old woman with an apparently milder form of CIPO characterized only by sporadic radiologically confirmed subocclusive episodes (i.e., air-fluid levels in distended bowel loops). Digestive symptoms are associated with malnutrition and amenorrhea. Endoscopy revealed long-segment (up to 14 cm) Barrett esophagus, intragastric bezoars, and megaduodenum. Functional tests provided results similar to those observed in her affected brothers, namely delayed gastric emptying and severe dysmotility (i.e., aperistalsis with simultaneous contractions, undetectable

lower esophageal sphincter pressure) at esophageal manometry. A male and female cousin, also born of consanguineous parents, were reported to have gastrointestinal complaints and died at 19 and 15 years of age, respectively. The female cousin who died at age 15 had clinical and radiologic evidence of CIPO, as well as renal hypoplasia, vesico-ureteral reflux, ascites and unspecified granulomatous hepatitis.

High-Throughput SNP genotyping

400 ng of genomic DNA from peripheral blood was used for high-throughput SNP genotyping on Illumina Infinium HD Assay Gemini platform (Illumina, San Diego, CA, USA), according to manufacturer's protocol. Genotypes were converted into PLINK format with custom scripts. PLINK v1.07 (http://ngu.mgh.harvard.edu/~purcell/plink/) was used to isolate individual Runs Of Homozygosity (ROH) that showed > 1 Mb overlap Mb overlap between the three affected siblings.

Whole Exome Sequencing (WES) analysis

1 μg of genomic DNA was subjected to a series of shotgun library construction steps, including fragmentation through acoustic sonication (Covaris, Woburn, MA, USA), end-polishing and A-tailing, ligation of sequencing adaptors and PCR amplification with 8 bp barcodes for multiplexing. Libraries underwent exome capture using the Roche/Nimblegen SeqCap EZ v3.0 (~62 MB target). Library quality was assessed by triplicate qPCR and molecular weight distributions verified on the Agilent Bioanalyzer (consistently 125 ± 15 bp). Pooled, barcoded libraries were sequenced via paired-end 50 bp reads with an 8 bp barcode read on Illumina HiSeq2000/2500 (RTA 1.13.48.0) sequencers (Illumina). Unaligned BAM files were aligned to a human reference (hg19) using BWA (Burrows-Wheeler Aligner; v0.6.2). Read data

from a flowcell-lane were treated independently for alignment and QC purposes before merging data to complete an exome. Sample-level QC was performed on merged data after it had met threshold for coverage metrics on exome target. Read-pairs not mapping within ± 2 standard deviations of the average library size (~125 ± 15 bp for exomes) were removed. All aligned read data were subject to the following steps: (1) removal of duplicate reads using Picard MarkDuplicates v1.70 (2) indel realignment with GATK (Genome Analysis Toolkit; https://www.broadinstitute.org/gatk/) IndelRealigner v1.6-11-g3b2fab9; (3) base qualities recalibration with GATK TableRecalibration; variants were flagged using the filtration walker (GATK) to mark sites that were of lower quality/false positives [e.g., low quality scores (Q50), allelic imbalance (ABHet 0.75), long homopolymer runs (HRun> 3) and/or low quality by depth (QD < 5)]. Variants were annotated with the SeattleSeq137 Annotation Server (http://gvs.gs.washington.edu/ SeattleSeqAnnotation).

RAD21 mutation screening in sporadic CIPO patients

PCR primers for human RAD21 (NM_006265.2) were designed with Primer3 v4.0 (http://primer3.ut.ee) and are available on request. Genomic DNA extracted from peripheral blood was amplified according to the following PCR conditions: 30 ng of DNA, 2.5 mM $MgCl_2$, 0.5 mM dNTPs, 0.5 μM primers, 5% DMSO in a final volume of 20 μl using the 2X KAPA Fast Taq Polymerase Master mix (KAPA Biosystems, MA, US). Forty cycles were carried out as follows: 95°C 1′, 95°C 15″, 58°C 1″, 72°C 1″, with a final extension of 30″at 72°C. PCR products were purified onto Millipore PCR clean-up plates and directly sequenced on both strands using the BigDye v1.1 kit (Life Technologies, Carlsbad, CA, USA). Electropherograms were visualized with Chromas version 2.0 and Sequencer version 4.7.

RAD21 cDNA transfection into HEK293 cells

Human *RAD21* cDNA inserted in pCMV6 vector in frame with DDK epitope was purchased from OriGene (OriGene, Rockville, MD, USA). The mutation corresponding to p.622 Ala>Thr was inserted by site-directed mutagenesis using the QuickChange XL mutagenesis kit (Agilent Technologies, Santa Clara, CA, USA) according to manufacturer's instructions. The insertion of the changes was verified by direct sequencing. $3x10^5$ HEK293 human renal cells (ATCC, UK) were plated for transfection of the different plasmids using liposomes according to manufacturer' instructions (Lipofectamine, Life Technologies). Protein and RNA extraction was performed after 48 hrs from transfection.

Gene expression analysis

Total RNA from 1.5 ml fresh blood was extracted with the QIAGEN Blood Total RNA kit (QIAGEN, Venlo, Limburg, Netherlands). Total RNA from $5x10^6$ LCLs or HEK293 cells, cultured according to standard protocols, was extracted with the RNeasy kit (QIAGEN). 1µg of *DNase I*-treated RNA was used for reverse transcription with random hexamers using the Multiscribe RT system (Life Technologies) at 48°C for 40′ in a final volume of 50 µl. qRT-PCR was performed with SYBRGreen, 0.5 µM primers, in an ABI 7500 Real-Time PCR System (Life Technologies). All target genes were normalized with the corresponding endogenous control (beta-actin) using the ΔΔCt comparative method. PCR primers are available on request.

Immunoprecipitation and western blotting

$2x10^6$ LCLs were lysed in 50 mM HEPES, 1 mM EDTA, 10% glycerol, 1% Triton X-100, 150 mM NaCl in presence of protease inhibitors (Roche Diagnostics, Basel, Switzerland) and phosphatase inhibitors (Inhibition Cocktails 2 and 3, Sigma, St.

Louis, MO, US). Pre-clearing was performed with rabbit IgG (Millipore, Billerica, MA, US) 1 hr at 4°C. Immunoprecipitation assays were performed at 4°C using 0.8 μg rabbit anti-SMC1 or anti-RAD21 antibody/reaction (Sigma Prestige) on Protein G-Sepharose (Sigma). Proteins were separated by SDS gel electrophoresis, transferred onto nitrocellulose membrane (GE Healthcare, Little Chalfont, UK) and subjected to western blotting with the Western Breeze kit (Life Technologies). Proteins extracted from sera of patients were diluted 1:5 in PBS, quantified with Lowry method and Coomassie Blue gel staining, separated by SDS gel electrophoresis, and transferred onto nitrocellulose membrane (GE Healthcare). Primary antibodies used were the following: goat anti-APOB48 1:250 (Santa Cruz, Texas; USA) and goat anti-APOB 1:1000 (Dako, Santa Clara, CA, US); rabbit anti-APOB100 (Abcam, Cambridge, UK) 1:200; mouse anti-GAPDH (Abcam) diluted at 1:5000. Bands were visualized by the ECL method (GE Healthcare).

Zebrafish functional assays

To determine the effect of *rad21a* suppression in zebrafish embryos, a splice blocking morpholino was designed by Gene Tools, LLC (Philomath, OR, USA), *rad21a* MO (AGGGTCTGCGTTCCTTGACTTCCAT), targeting the splice junction at the 3´ end of exon 2. A published *ret* MO (ACACGATTCCCCGCGTACTTCCCAT) was used.[20] To measure *rad21a* MO efficiency, total mRNA was extracted from control and MO injected embryos, reverse-transcribed and the site targeted by the MO was PCR amplified using primers GGGACAAAAAGCTGACCAAA and CAGGGTGAACTGCTGTGCTA.

For knockdown and rescue experiments, we injected either 3ng of *rad21* MO (*runx1* expression), or 1.2 ng *rad21* MO (gut phenotype). For zebrafish injections, capped human *RAD21* mRNA was produced by cloning wild-type *RAD21* cDNA and the

three mutant constructs (P376R, C585R, and A622T) into the pCS2+ expression vector and reverse transcribing each construct *in vitro* with the SP6 Message Machine kit (Ambion, CA, US).

Injected embryos were fixed at 5 days post fertilization (dpf) in 4% PFA 16 hours at 4°C, and moved to methanol at -20°C. Following rehydration steps in decreasing series of methanol/PBT, permeabilization, post-fixation, and blocking, embryos were incubated with anti-HuC/D antibody (1:500; Life Technologies) 16 hours at 4°C. Following washes in PBT embryos were incubated with Alexa-488 (1:500, Invitrogen, Carlsbad, CA, US) secondary antibody. All experiments were repeated three times and a Pearson's chi-square test ($\chi 2$) was used to determine significance.

For *in situ* analysis, a *runx1* probe was designed using the following primers: AATTAACCCTCACTAAAGGGGCCACTGCAAGCACCTCTGG and TAATACGACTCACTATAGGACGAGGAGAGGACACAAAGC. Digoxigenin-labeled antisense probe was synthesized using T7 from a plasmid kindly provided by Kathryn Crosier. Injected embryos (~14dpf) were fixed in 4% paraformaldehyde 16 hours at 4°C and moved to 100% methanol for storage. After step-wise rehydration washes, embryos were incubated at 65°C with the *runx1* probe. Anti-digoxigenin antibodies conjugated with alkaline phosphatase antibody were used and developed with NBT/BCIP as substrate.

Electromobility shift assay (EMSA)

$2x10^6$ LCLs were rinsed in cold PBS-Na_3VO_4 0.2 mM, pelleted by centrifugation at 1600xg and lysed in 400 µl of Buffer A (10 mM HEPES pH 7.9, 10 mM KCl, 0.1mM EDTA, 1 mM DTT, 1 mM Na_3VO_4 and a protease inhibitors cocktail) for 15 min in ice. 25 µl of 10% NP-40 were added and the samples were centrifuged at 16000xg 30 sec. The nuclear pellets were resuspended in 50 µl Buffer C (20 mM HEPES pH 7.9,

0.4 mM KCl, 0.1mM EDTA, 0.1 mM EGTA, 1 mM DTT, 1 mM Na_3VO_4 and a protease inhibitors cocktail), incubated on ice for 45 min, and centrifuged at 16000xg 10 min at 4°C.10 µg of nuclear extracts, 20 fmol of biotin-labelled probes, 2 µg of sheared salmon sperm DNA, 2.5% glycerol, 5 mM KCl and 5 m$MgCl_2$ were incubated at room temperature for 30 min in 20 µl. Cold probes were added at a concentration 200X. The nuclear complexes were resolved by non-denaturing electrophoresis on 4% polyacrilammide gel, transferred onto nitrocellulose membrane at 380 mA 30 min at 4°C, crosslinked via UV binding 15 min at room temperature. For supershift assay, nuclear extracts were incubated at the same conditions as reported above, but the complexes were immunoprecipitated 40 min at 4°C with 1.5 µg of rabbit anti-RAD21 antibody (Abcam) before the EMSA assays. Complexes were resolved under non-denaturing conditions using a 3.5% polyacrylamide gel. EMSA shift was revealed with the LightShift Chemiluminescent EMSA Kit (Thermo Scientific Inc., IL, US). The used biotin-labelled probes are the following: hAPO_AC2 5′- ACGGAGTTGTCAAGGCGGGGGCTGCAGGCAGAGGGCGCTAAAGAGCCCA GGATGGCCGGG-3′ (chr11:116,662,104-116,662,163, hg19); hAPOB_c1 5′- CAGAGCACTGAAGACGCTTGGGGAAGGGAACCCACCTGGGACCCAGCCC CTGGTGGCTGCGGCTGCAT-3′ (chr2:21,267,106-21,267,173, hg19) ; hAPOB_c2 5′- CATTCCCACCGGGACCTGCGGGGCTGAGTGCCCTTCT-3′ (chr2:21,266,910-21,266,946, hg19).

Immunohistochemistry

Immunohistochemistry was performed on paraffin-embedded adult human colon tissues (patients routinely operated for uncomplicated colon cancers commonly used as controls for immunohistochemical experiments) according to protocols validated in

our laboratory. Briefly, tissue sections were treated to remove paraffin embedding by three sequential washes in xylene and graded ethanol. Antigen unmasking was performed by heating sections at 95°C in 10 mM Sodium citrate buffer, pH 6.0, for 10 min and subsequent cooling at room temperature for 30 min. To reduce endogenous peroxidases, tissue sections were treated with an ad hoc blocking kit (GeneTex Inc., Irvine, CA; USA) and incubation for 16 h at 4°C with primary antibodies. The following primary antibodies were used: anti-human APOB48 (Santa Cruz) and anti-human APOB diluted 1:100 (Abcam); anti-human RAD21 diluted 1:250 (Sigma Prestige), anti-human APOBEC1 diluted 1:100 (Creative Diagnostics, Bristol, UK). Incubations with the corresponding blocking peptides or with the secondary antibodies only were performed as negative controls (Supplementary Figures 2a, b). Fluorescent secondary antibodies were diluted 1:300 in Triton-X and incubated 60 min at room temperature, before subsequent dehydration and visualization under a LEICA DMLB fluorescent microscope. DAB staining was performed according to standard protocols.

Quantitative evaluation of ganglion cells

We counted the number of neurons after immunostaining with a rabbit polyclonal anti human neuronal specific enolase (NSE) antibody 1:400 (Millipore, Germany). For each section, 25-28 high power (40x) microscopic fields, along the neuromuscular ridge of the myenteric ganglia, were captured to assess NSE immunoreactive neuronal cell bodies / ganglion.[22] The same procedure was performed for the counts of neurons in the submucosal ganglia. Sections were examined using a Leica microscope equipped with a digital camera.

Supplementary Table 1: Individual and shared ROH in the 3 affected siblings.

ID	Chr	Start (SNP)	End (SNP)	Start (bp)	End (bp)	Length (Kb)	N° SNPs
IV-9	8	rs2737227	rs6998986	116713296	124956205	8242.91	864
IV-10	8	rs2737227	rs6998986	116713296	124956205	8242.91	864
IV-11	8	rs2737227	rs6998986	116713296	124956205	8242.91	864
Overlap	8	rs2737227	rs6998986	116713296	124956205	8242.91	864
IV-11	8	rs6471254	rs1420849	91878147	113307176	21429	2043
IV-10	8	rs1850819	rs1420849	78905837	113307176	34401.3	2964
IV-9	8	rs2622590	rs1420849	56520828	113307176	56786.3	5025
Overlap	8	rs6471254	rs1420849	91878147	113307176	21429	2043

Supplementary Table 2: Cholesterol and HDL levels in CIPO. Normal values: cholesterol ≤ 200; HDL ≥ 35.

Patient reference code	Sex	Total cholesterol	HDL
ITA_CIPO08	M	158	59
ITA_CIPO27	F	154	64
ITA_CIPO37	F	150	53
ITA_CIPO23	M	200	42
ITA_CIPO38	F	168	80
ITA_CIPO29	M	202	49
ITA_CIPO39	F	142	41
ITA_CIPO26	F	181	51
ITA_CIPO24	F	198	48
ITA_CIPO16	F	150	52
ITA_CIPO14	F	200	53
ITA_CIPO33	M	126	25
ITA_CIPO30	F	201	76

Legend to Supplementary Figures

Supplementary Figure 1. RT-PCR analysis of knockdown efficiency for splice-site targeted *rad21* Morpholino. (**A**) Schematic of zebrafish *rad21*. A splice blocking MO (red bar) was designed against the second exon-intron junction. PCR primers (blue bar) designed against exon 1 and exon 3 were used to test MO

efficiency. (**B**) In control embryos, there is a single amplicon, while in *rad21* MO, there are two amplicons, demonstrating the efficiency of the MO used.

Supplementary Figure 2. Serial dilutions for APOB48 western blotting and negative controls for immunohistochemistry analysis: (**A**) serial dilutions of sera from CIPO patients and controls; images are representative of replica experiments; (**B-C**) images of negative controls, including primary antibody omission and blocking with the corresponding peptides for APOB (**B**) and RAD21 (**C**) are shown.

Supplementary Figure 3. Functional studies of RAD21 mutation p.622Ala>Thr *in vitro*. (A) Screenshot of the parallel sequencing output for the mutation in RAD21 (genomic change). (**B,C**) *RAD21* expression is not altered in patient's blood (**B**) and lymphoblastoid cell lines (**C**). RAD21 expression was evaluated by real-time qRT-PCR; (**D**) *RAD21* expression immunoprecipitation analysis for SMC1 and RAD21 from protein extracts of LCLs, showing that the binding is retained even in presence of the mutated protein (second lane in each panel). (**E**) RT-qPCR for *RUNX1* expression in HEK293 cells transfected either with empty, RAD21 wild-type, RAD21 mutant p.622 Thr vectors. Data represent the mean values of three independent transfection experiments. Bars represent the standard deviation; black asterisk indicates the significant p-value. (Representative western blotting analysis of recombinant RAD21 in frame with the DDK epitope in the transfected cells is reported in main Figure 4C). (**F**) EMSA analysis showing that LCL nuclear extracts containing either RAD21 wild-type or mutant protein retain the binding ability for the AC2 site on chromosome 11. Black arrows indicate the gel-shifts.

Supplementary Figure 4. EMSA assays showing the RAD21-specific supershifts for the two regions in human APOB promoter. Black arrows indicate the shift, grey stars indicate the supershift observed only in lanes derived from control's

nuclear extracts. For the c_1 region the complexes in the supershift were resolved only after a longer gel run, without keeping into the gel the free biotin-labelled probes. Images are representative of three independent experiments.

Supplementary Figure 5. Western blotting for APOB on CIPO and IBS sera. (**A**) Western blotting analysis of APOB100 in sera of CIPO patient carrying RAD21 mutation, controls and CIPO patients; (**B**) Immunoblots showing the increased expression of APOB48 in sera of the CIPO patients included in RAD21 mutation screening, compared to controls; (**C)** Immunoblots for APOB48 in IBS vs CIPO patients and controls. Abbreviations are as shown in Figure 5. In bold are represented the samples loaded in different gels and analysed for APOB48 expression.

Supplementary Figure 6: **RAD21 and APOBEC1 immunostaining**. Figures (**A**-i to iv) show RAD21 immunoreactivity in gut biopsies of controls (**A**-i, iii) and CIPO patients (**A**-ii, iv). The representative pictures indicate RAD21 immunolabeling in the nuclei of epithelial and *lamina propria* immunocyte-like cells (**A**-i, ii) as well as myenteric neurons (**A**-iii, iv). Figures (**B**i-ii) illustrate APOBEC1 labeling with an overlapping immunoreactive pattern to that observed for RAD21, showing no changes in controls (**B**-i) and CIPO patients (**B**-ii).

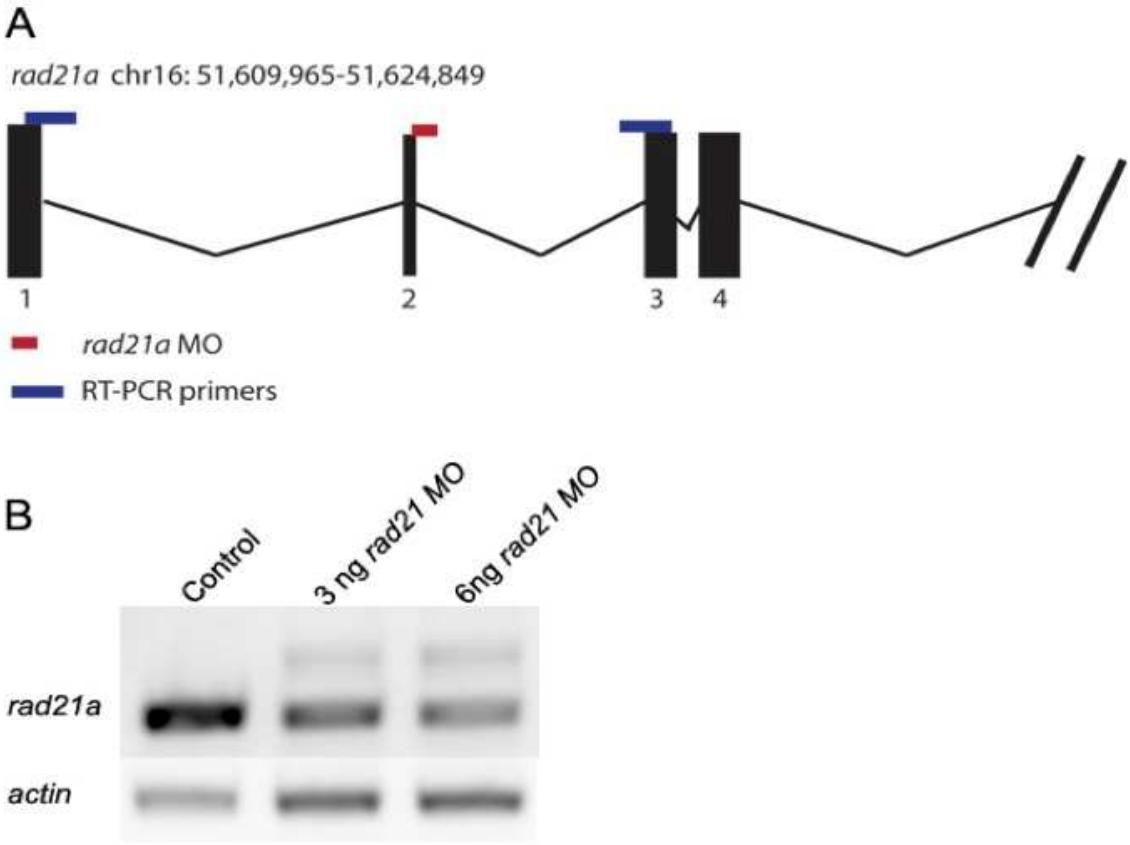
A
rad21a chr16: 51,609,965-51,624,849
1
2
3
4
rad21a MO
RT-PCR primers
B
Control
3 ng rad21 MO
6ng rad21 MO
rad21a
actin

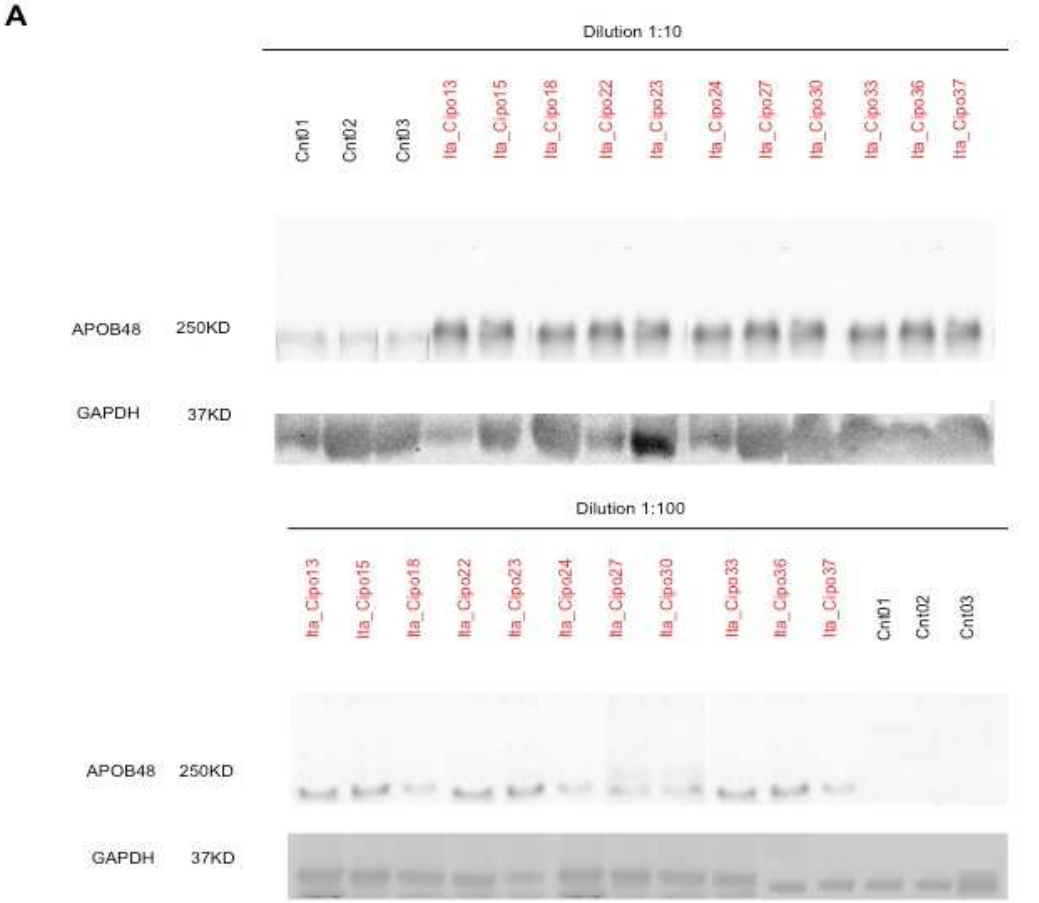
A
Dilution 1:10
Cnt01
Cnt02
Cnt03
Ita_Cipo13
Ita_Cipo15
Ita_Cipo18
Ita_Cipo22
Ita_Cipo23
Ita_Cipo24
Ita_Cipo27
Ita_Cipo30
Ita_Cipo33
Ita_Cipo36
Ita_Cipo37
APOB48 250KD
GAPDH 37KD
Dilution 1:100
Ita_Cipo13
Ita_Cipo15
Ita_Cipo18
Ita_Cipo22
Ita_Cipo23
Ita_Cipo24
Ita_Cipo27
Ita_Cipo30
Ita_Cipo33
Ita_Cipo36
Ita_Cipo37
Cnt01
Cnt02
Cnt03
APOB48 250KD
GAPDH 37KD

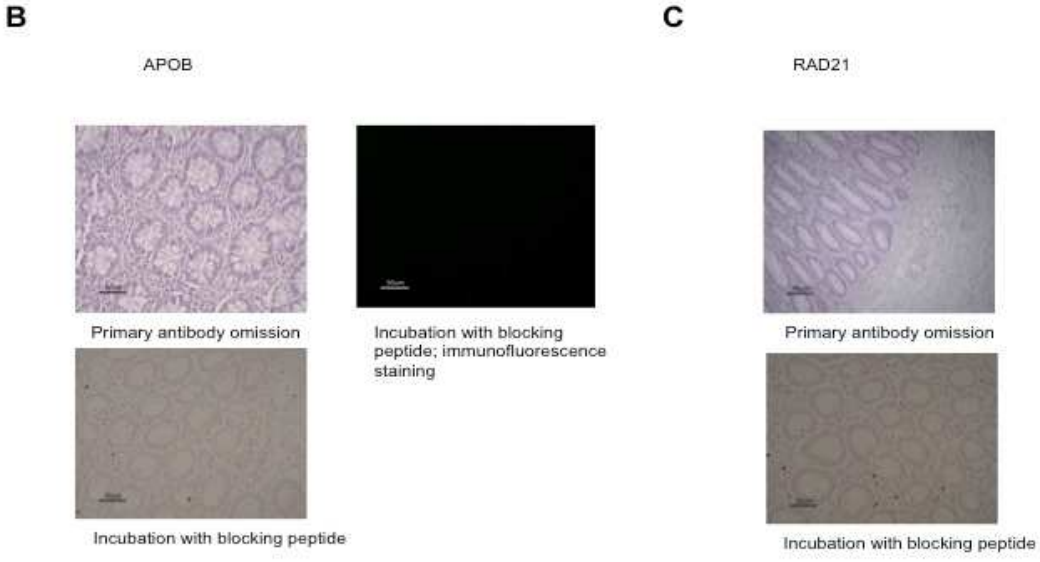
B
APOB
Primary antibody omission
Incubation with blocking peptide; immunofluorescence staining
Incubation with blocking peptide
C
RAD21
Primary antibody omission
Incubation with blocking peptide

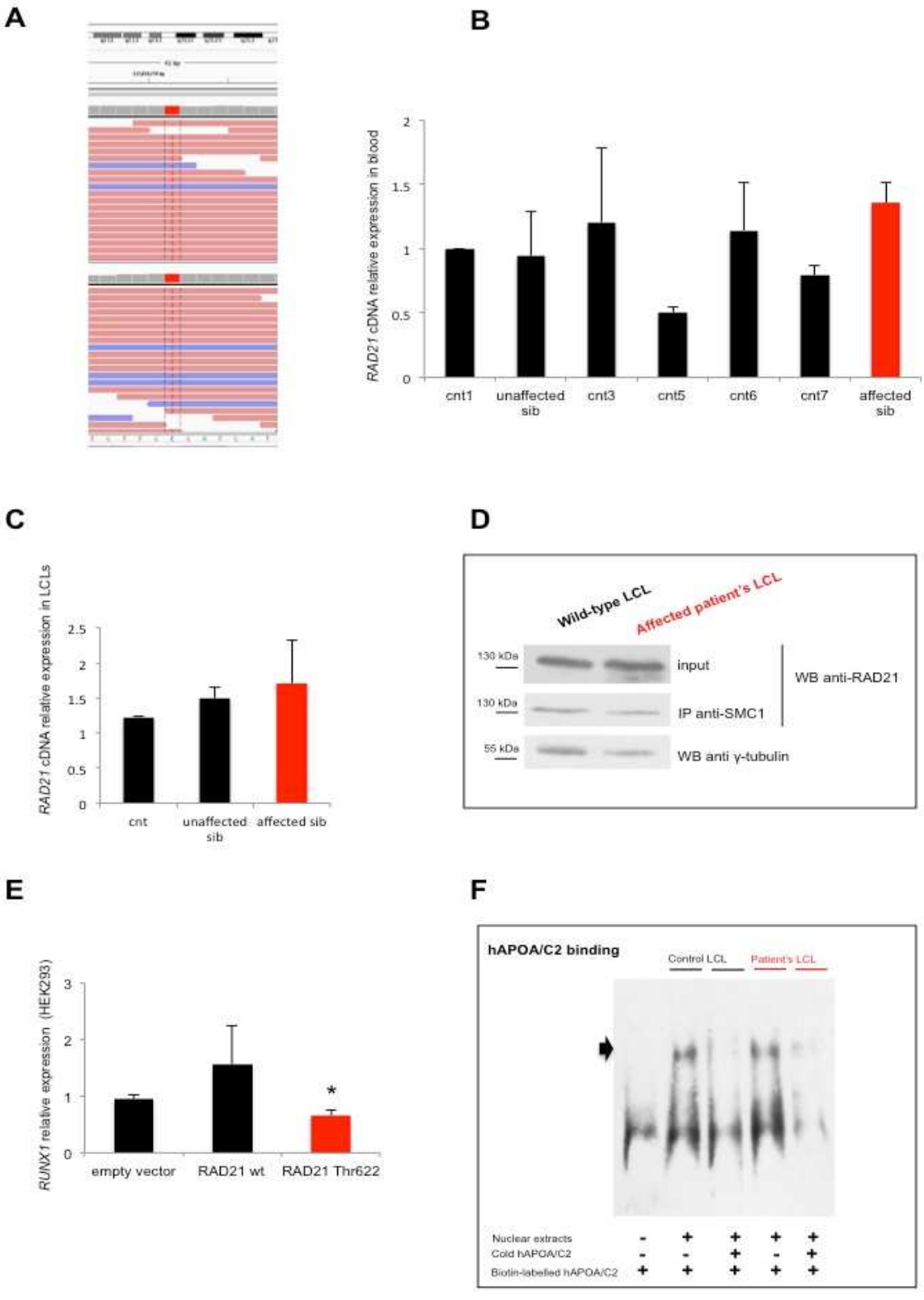
A
B
RAD21 cDNA relative expression in blood
2
1.5
1
0.5
0
cnt1
unaffected sib
cnt3
cnt5
cnt6
cnt7
affected sib
C
RAD21 cDNA relative expression in LCLs
2.5
2
1.5
1
0.5
0
cnt
unaffected sib
affected sib
D
Wild-type LCL
Affected patient's LCL
130 kDa
input
WB anti-RAD21
130 kDa
IP anti-SMC1
55 kDa
WB anti γ-tubulin
E
RUNX1 relative expression (HEK293)
3
2
1
0
*
empty vector
RAD21 wt
RAD21 Thr622
F
hAPOA/C2 binding
Control LCL
Patient's LCL
Nuclear extracts - + + + +
Cold hAPOA/C2 - - + - +
Biotin-labelled hAPOA/C2 + + + + +

A

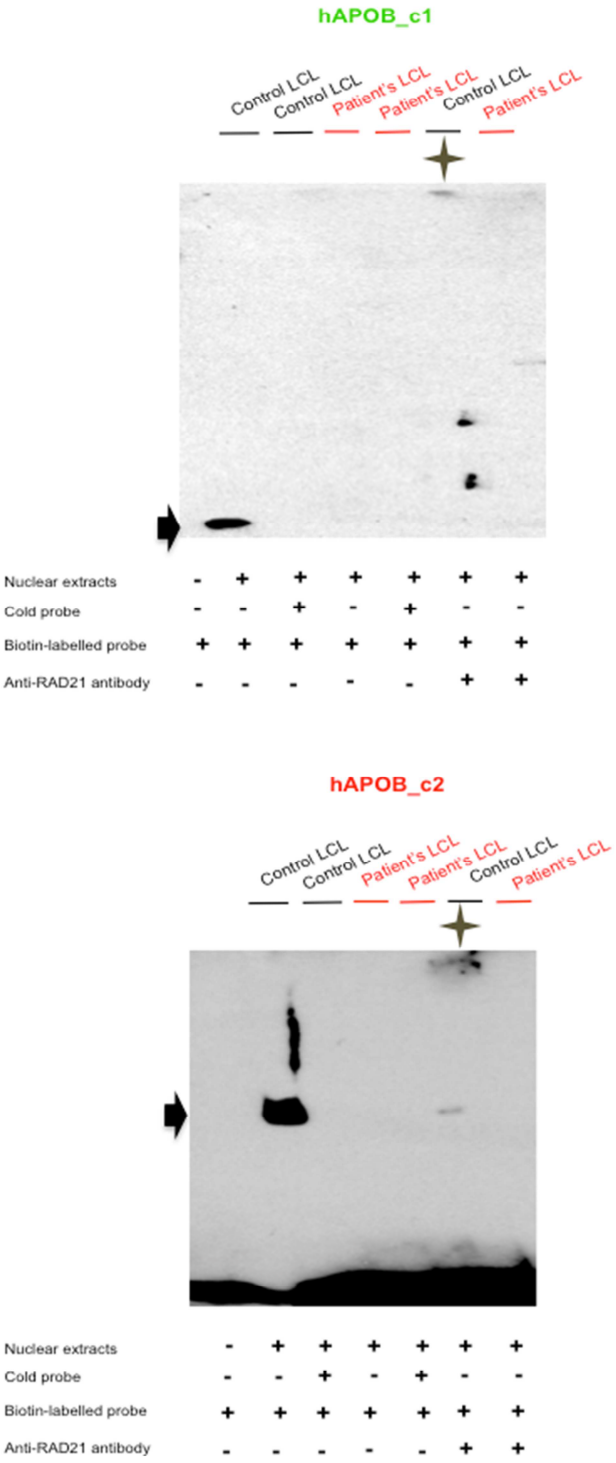
hAPOB_c1
Control LCL
Control LCL
Patient's LCL
Patient's LCL
Control LCL
Patient's LCL
Nuclear extracts - + + + + + +
Cold probe - - + - + - -
Biotin-labelled probe + + + + + + +
Anti-RAD21 antibody - - - - - + +
hAPOB_c2
Control LCL
Control LCL
Patient's LCL
Patient's LCL
Control LCL
Patient's LCL
Nuclear extracts - + + + + + +
Cold probe - - + - + - -
Biotin-labelled probe + + + + + + +
Anti-RAD21 antibody - - - - - + +

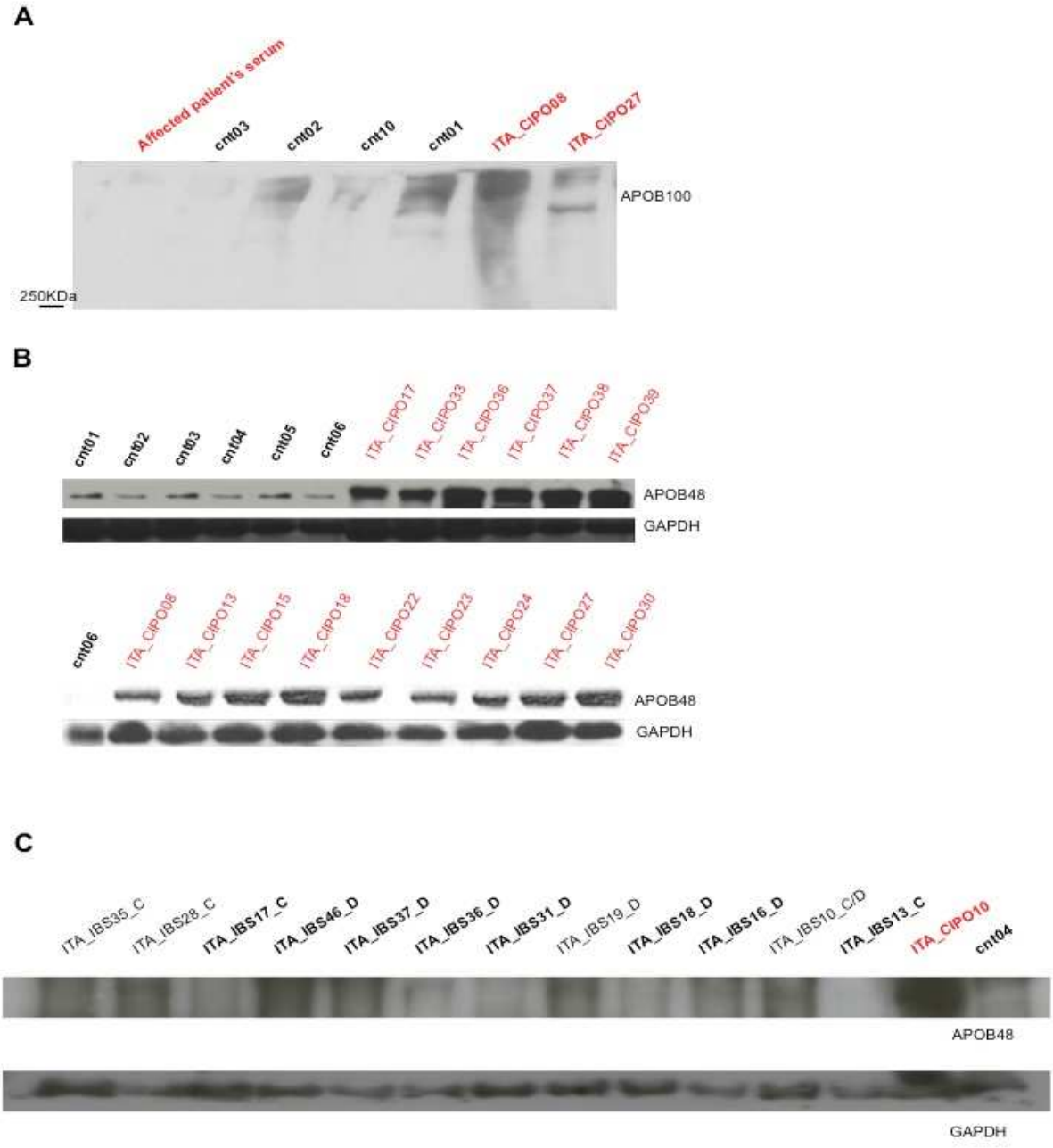
A
Affected patient's serum
cnt03
cnt02
cnt10
cnt01
ITA_CIPO08
ITA_CIPO27
APOB100
250KDa
B
cnt01
cnt02
cnt03
cnt04
cnt05
cnt06
ITA_CIPO17
ITA_CIPO33
ITA_CIPO36
ITA_CIPO37
ITA_CIPO38
ITA_CIPO39
APOB48
GAPDH
cnt06
ITA_CIPO08
ITA_CIPO13
ITA_CIPO15
ITA_CIPO18
ITA_CIPO22
ITA_CIPO23
ITA_CIPO24
ITA_CIPO27
ITA_CIPO30
APOB48
GAPDH
C
ITA_IBS35_C
ITA_IBS28_C
ITA_IBS17_C
ITA_IBS46_D
ITA_IBS37_D
ITA_IBS36_D
ITA_IBS31_D
ITA_IBS19_D
ITA_IBS18_D
ITA_IBS16_D
ITA_IBS10_C/D
ITA_IBS13_C
ITA_CIPO10
cnt04
APOB48
GAPDH

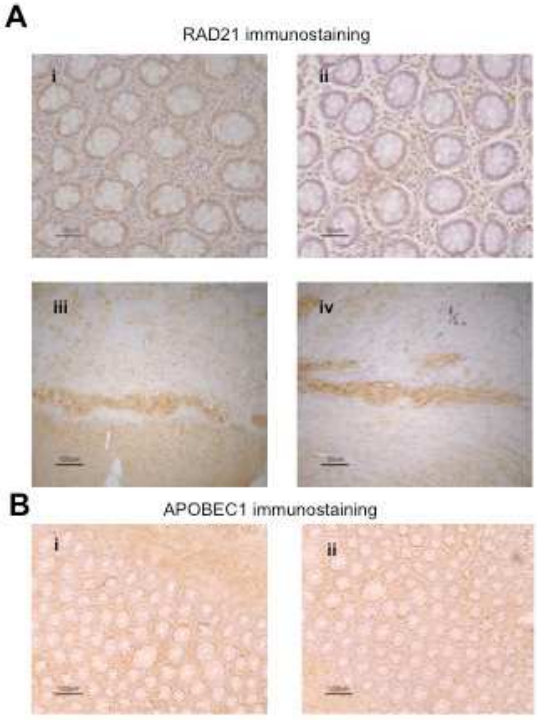
A
RAD21 immunostaining
i
ii
iii
iv
B
APOBEC1 immunostaining
i
ii

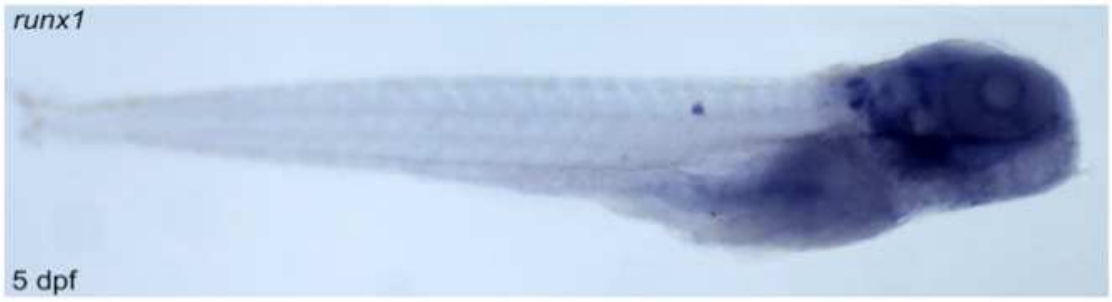
runx1
5 dpf